

A. KRZĄKAŁA\*, J. MLYŃSKI\*, G. DERCZ\*\*, J. MICHALSKA\*\*\*, A. MACIEJ\*\*, Ł. NIEUŻYŁA\*\*, W. SIMKA\*\*

## MODIFICATION OF Ti-6Al-4V ALLOY SURFACE BY EPD-PEO PROCESS IN ZrSiO<sub>4</sub> SUSPENSION

### MODYFIKACJA POWIERZCHNI STOPU Ti-6Al-4V METODĄ PEO-EPD W ZAWIESINIE ZrSiO<sub>4</sub>

Investigations on the surface modification of the Ti-6Al-4V alloy by plasma electrolytic oxidation are reported here. The oxidation process was carried out in a solution containing a zirconium silicate (ZrSiO<sub>4</sub>) suspension and sodium hydroxide (NaOH). Anodising was realised at voltages in a range from 100 V to 250 V. It was found that the morphology of the sample surface did not change during the oxidation of the alloy at 100 V. Application of voltages higher than 100 V led to the incorporation of zirconium silicate into the formed oxide layer and to significant changes of the surface morphology.

*Keywords:* Ti-6Al-4V alloy, suspension, anodic oxidation, zirconium silicate

W pracy przedstawiono wyniki badań nad modyfikacją powierzchni stopu Ti-6Al-4V metodą plazmowego utleniania elektrochemicznego. Proces ten prowadzono w roztworze zawierającym zawiesinę krzemianu cyrkonu (ZrSiO<sub>4</sub>) oraz wodorotlenek sodu (NaOH). Anodowanie prowadzono w zakresie napięcia od 100 do 250 V. Stwierdzono, że zastosowanie napięcia 100 V nie powoduje zmian w morfologii powierzchni stopu. Natomiast zastosowanie napięcia wyższego od 100 V powoduje wbudowanie krzemianu cyrkonu w tworzącą się warstwę tlenową oraz znaczne zmiany w morfologii powierzchni stopu Ti-6Al-4V.

### 1. Introduction

Metals and their alloys are the most popular materials for orthopaedic implants. The special place is occupied by titanium and its alloys due to their high biocompatibility, good strength to weight ratio, good corrosion resistance and mechanical behavior [1-3]. Titanium and its alloys are used mainly in aerospace, marine, biomedicine, etc. [2]. The most popular titanium alloy for orthopaedic implants production is Ti-6Al-4V, which originally was dedicated for aerospace applications. It still occupies about 50% of all titanium tonnage in the world [4], despite new vanadium-free alloys occurring. On the surface of titanium alloys the oxide layer of TiO<sub>2</sub> is formed spontaneously [4]. In body environment complex reactions take place. Stability of oxide passive layer is very important then, due to possibility of release vanadium ions to the body fluids. Vanadium is considered as potentially cytotoxic [5], so other titanium alloys, tailored to biomedical applications, were obtained. The first generation alloys contain Nb or Fe and have similar properties to Ti-6Al-4V. The second generation implants contain Mo, Zr, Ta, Pd and Sn. Among of them the Ti-13Nb-13Zr alloy becomes more popular. It is considered as "completely biocompatible" because of presence Nb and Zr elements [1]. These elements in oxidative environment tend to form sparingly soluble oxides, similarly to titanium,

what prevent releasing of the metals ions into body fluids. Zirconium (Zr) is widely used to obtain prosthetic devices due to its good mechanical properties and biocompatibility. The results of many studies indicate that Zr implants exhibit excellent osseointegration and zirconium-related materials, such as zirconia ceramics and coatings, have previously been used as bone implant materials [6-8]. Even small amount of zirconia enhances mechanical properties of hydroxyapatite [6]. Also the zirconium silicate can be used to introduce zirconium and silicon to the metallic implant. Silicon is an important element for growth and development bones and connective tissues [9]. Concentration of silicon is observed to be highest at the earliest stages of calcification, and with more advanced mineralization Si concentration decreases [10]. Silicon in form of orthosilicic acid (Si(OH)<sub>4</sub>) is able to induce the precipitation of hydroxyapatite even in the presence of proteins, that normally inhibit its precipitation [10]. Incorporation of different elements is used to improve biocompatibility of metallic implants and there is many ways to achieve this aim, e.g. physical vapour deposition/chemical vapour deposition, laser nitriding, anodizing, sol-gel method, plasma electrolytic oxidation [11] and electrophoretic deposition (EPD) [12]. Electrophoretic deposition is widely used in the processing of advanced ceramics and coatings. EPD is the colloidal process based on the suspension of particles in a solvent [13]. Depending on which

\* FACULTY OF CHEMISTRY, SILESIA UNIVERSITY OF TECHNOLOGY, 6 KRZYWOSTEGO STR., 44-100 GLIWICE, POLAND

\*\* INSTITUTE OF MATERIALS SCIENCE, UNIVERSITY OF SILESIA, 75 PUŁKU PIECHOTY STR.1A, 41-500 CHORZÓW, POLAND

\*\*\* FACULTY OF MATERIALS SCIENCE AND METALLURGY, SILESIA UNIVERSITY OF TECHNOLOGY, 8 KRASIŃSKIEGO STR., 40-019 KATOWICE, POLAND

electrode to deposition is used one can distinguish two types of EPD: cathodic electrophoretic process (particles positively charged) or anodic electrophoretic deposition process (negatively charged particles). Process is used to obtaining wear resistant and anti-oxidant ceramic coatings fabrication of functional films for microelectronic devices and solid oxide fuel cells, and also development of novel bioactive composites or coating for medical implants and nanoscale advanced functional materials [12].

In this study possibility of electrophoretic deposition – plasma electrolytic oxidation method (EPD-PEO) for the Ti-6Al-4V alloy surface modification in ZrSiO<sub>4</sub> suspension for the first time was presented. Influence of ZrSiO<sub>4</sub> and NaOH concentration was investigated. For obtained materials, SEM, EDX and XRD analysis as well as profile measurements were conducted.

## 2. Materials and methods

The Ti-6Al-4V alloy (BIMO Metals, Wrocław, Poland) was used as a substrate material. Chemical composition of this alloy is presented in Table 1. Sample surface area equals 4.24 cm<sup>2</sup>. Pretreatment of samples was conducted as follows: polishing with abrasive papers of 320, 600 and 800 granulation, etching in a solution containing H<sub>2</sub>SO<sub>4</sub> (4 mol dm<sup>-3</sup>) and HF (1 mol dm<sup>-3</sup>) for 1 min, rinsing in deionised water and ultrasonically cleaning for 5 min.

TABLE 1  
The chemical composition of the Ti-6Al-4V alloy

C	H	N	O	Fe	Al	V	Ti
0.024	0.005	0.006	0.18	0.17	6.0	4.1	balance

All of the solutions were prepared using analytical grade reagents manufactured by POCh, Gliwice

### The EPD-PEO process

The EPD-PEO process was carried out with a DC power supply (PWR800H, Kikusui, Japan), and cooled electrolyser. The anode was Ti-6Al-4V alloy specimen and the cathode was a titanium mesh. Time of anodising was 5 min. The baths composition is presented in Table 2. The sample labels and treatment conditions are presented in Table 3.

TABLE 2  
The chemical composition of baths used in the EPD-PEO process

Bath	Components, g dm <sup>-3</sup>	
	ZrSiO <sub>4</sub>	NaOH
A	10	5
B	50	
C	100	10
D		
E		
F	200	5

TABLE 3

The sample labels, process conditions, and influence of its on the roughness factor Ra and Zr/Si atomic ratio

Bath	Sample	Parameters		Ra, μm	Zr/Si
		Voltage, V	Current density, mA cm <sup>-2</sup>		
A	A1	200	100	0.72	0.71
	A2	250	100	3.36	0.82
B	B1	200	100	0.53	0
	B2	250	100	0.57	0.60
C	C1	100	100	0.17	0.73
	C2	200	50	0.13	0.64
	C3	200	100	0.18	0.89
	C4	200	200	0.16	0.93
	C5	200	500	0.17	0.82
	C6	250	100	0.20	0.81
D	D1	200	100	2.93	0.88
	D2	250	100	4.28	0.79
E	E1	200	100	3.94	0.99
	E2	250	100	3.06	0.96
F	F3	200	100	0.17	0.45
	F4	250	100	0.35	0.58

### The SEM and EDX analysis

The morphology and chemical composition of the anodic layer formed on the Ti-6Al-4V alloy surface were examined using a scanning electron microscope (SEM, Hitachi S-3400N, accelerating voltage = 25 kV) and an energy-dispersive X-ray spectrometer (EDX, Thermo Noran) attached to the SEM. EDX spectra were collected from whole sample surface.

### XRD investigations

The X-ray diffraction experiments were performed on an X-Pert Philips PW 3040/60 diffractometer operating at 30 mA and 40 kV, which was equipped with a vertical goniometer and Eulerian cradle. The wavelength of radiation ( $\lambda_{CuK\alpha}$ ) was 1.54178 Å. The grazing incidence X-ray diffraction (GIXD) patterns were registered in the  $2\theta$  range from 10° to 80° with a 0.05° step for the incident angle  $\alpha$ : 0.25 degree.

### The surface roughness investigations

The roughness (Ra parameter) of the samples was measured using a Mitutoyo SurfTest SJ-301 profilometer according to the EN ISO 4287:1997 standard.

## 3. Results and discussion

The influence of ZrSiO<sub>4</sub> and NaOH concentration as well as current density and applied voltage on morphology and composition of obtained coatings were determined. The morphology of etched Ti-6Al-4V alloy is presented in Fig. 1. shows the morphology of sample treated in A bath (10 g dm<sup>-3</sup> ZrSiO<sub>4</sub> and 5 g dm<sup>-3</sup> NaOH). The surface of the sample changed in comparison to sample etched only (Fig. 1). Scratches after polishing are still visible but surface is covered with the thin film, there are also some not uniformly distributed

particles on the surface. When applied voltage increased from 200 to 250 V on the surface of examined sample more  $ZrSiO_4$  particles occurred (Fig. 2). Also small pores typical for PEO are visible. The EDX spectrum shows the presence of titanium alloy's elements and confirmed incorporation of Zr and Si to the surface layer, with increase of voltage also amount of incorporated elements increased. Also XRD analysis confirmed

those results. On Fig. 3 XRD pattern prepared for A sample is presented. On the surface of sample crystalline phases of Ti,  $TiO_2$  and  $ZrSiO_4$  are seen. Peaks of Ti come from titanium substrate. Presence of  $TiO_2$  is the effect of PEO – titanium was oxidised to titania, and finally peaks of  $ZrSiO_4$  confirmed its incorporation from suspension to the oxide layer. Increase of  $ZrSiO_4$  suspension concentration from 10 to 50 g  $dm^{-3}$  (bath B) changed in morphology of the samples surface. Sample B1 anodised at 200 V is covered with the film of deposit and some particles not uniformly distributed (SEM image not presented). Anodisation at 250 V (sample B2-Fig. 4) caused uniformly porous structure with single particles on it. EDX analysis shows the presence of Zr and Si only in case of sample B2, not B1 – there is only Si peak(not presented). Peaks are small, also the presence of Na in surface layer was stated. Results of XRD analysis (not presented here) were similar to those of A sample.

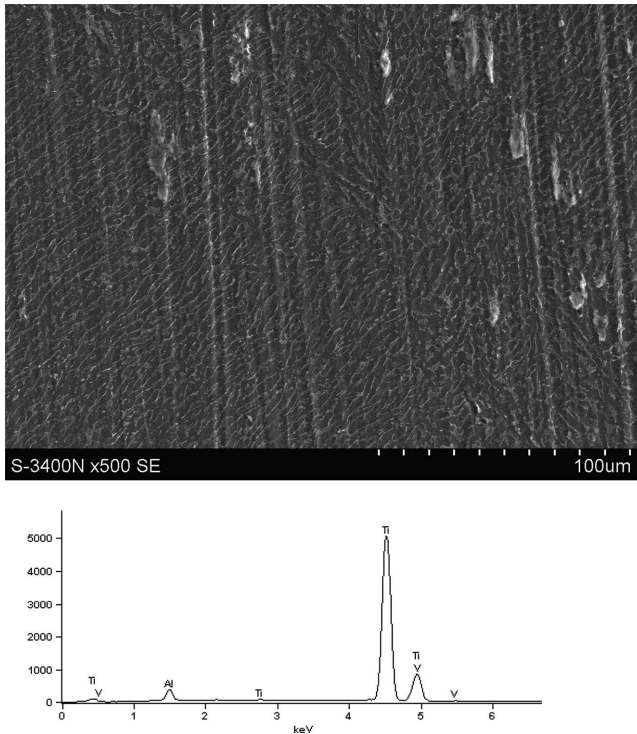


Fig. 1. The SEM image and the EDX spectrum of etched Ti-6Al-4V alloy sample

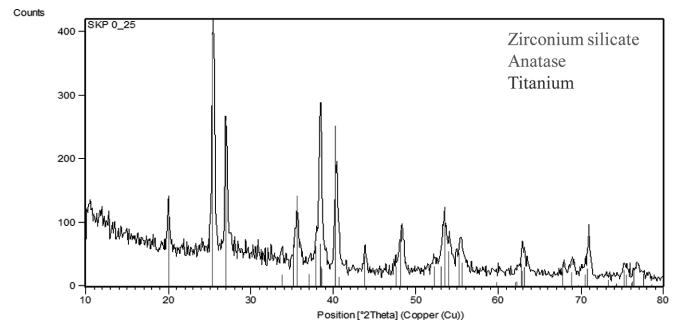


Fig. 3. XRD pattern of sample A2

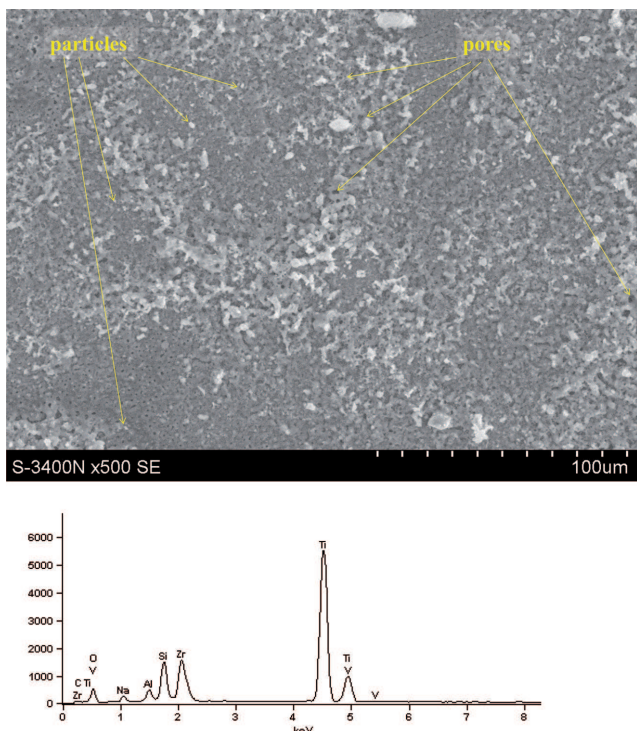


Fig. 2. The SEM image and the EDX spectrum of A2 sample

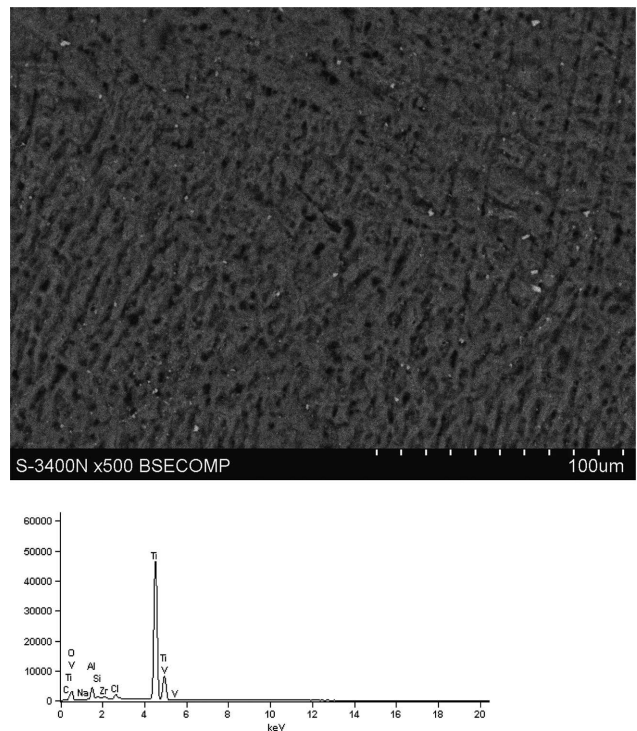


Fig. 4. The SEM image and the EDX spectrum of B2 sample

In case of samples labeled as C, investigations were carried out in bath C enriched in  $ZrSiO_4$  (100 g  $dm^{-3}$ ). The surface of sample C1 was similar to sample A1, scratches after polishing remained, but more particles were incorporated

into the surface. When applied voltage increased (from 100 to 200 V) more porous structure was obtained (Fig. 5). Moreover, decreasing of current density from 100 to 50 mA cm<sup>-2</sup> could caused less intense particles incorporation. In case of samples C2-C5 increasing the current density increased amount of particles on the surface. Whereas, increase of voltage to 250V not caused desirable changes – structure (C6 vs. C3) is dense and less amount of particles occurs. EDX spectra of examined samples are quite similar each other - substrate elements were detected and small peaks from Si and Zr, in the case of sample C4 atomic ratio Zr/Si equals 0.93. Ra parameter of layers vary from 0.13 to 0.20 μm (Table 3).

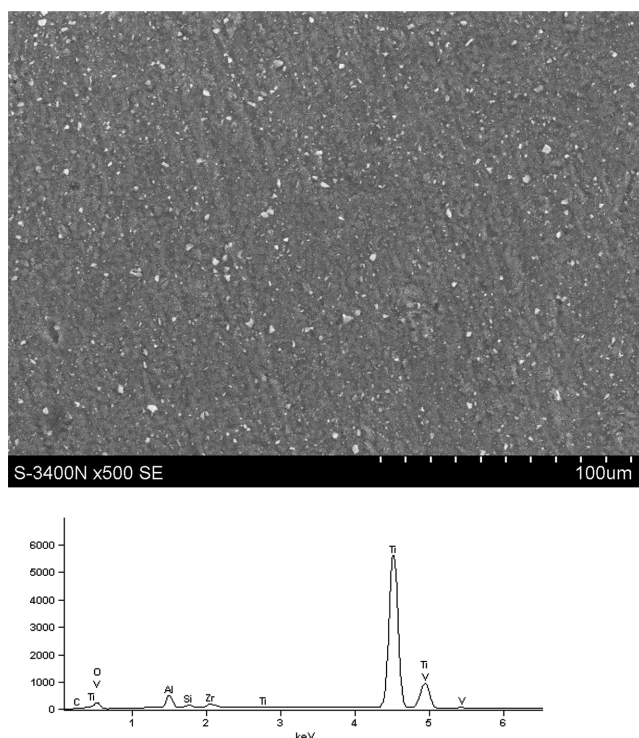


Fig. 5. The SEM image and the EDX spectrum of C4 sample

More alkaline environment (10 g dm<sup>-3</sup> NaOH) improved the incorporation of Zr and Si. Increase of applied voltage caused changes in obtained layers (samples D1 and D2). When process was performed at 200 V (sample D1 – Fig. 6) more uniform structure of incorporated species occurred then at 250 V. EDX spectra also show that amount of Zr and Si is higher when lower voltage was used (Table 3). XRD spectrum prepared for D sample shows the presence of ZrSiO<sub>4</sub> in the surface layer and also SiO<sub>2</sub> and ZrO<sub>2</sub> (Fig. 7, 9). In alkaline environment ZrSiO<sub>4</sub> could hydrolyse and in the bath there are not only particles of ZrSiO<sub>4</sub>, but also of ZrO<sub>2</sub> and dissolved Na<sub>2</sub>SiO<sub>3</sub>. When zirconia particles are present in sodium silicate electrolyte [13], after the process on the surface layer of the sample presence of ZrSiO<sub>4</sub> was not confirmed. Authors stated that the ZrSiO<sub>4</sub> is formed in the ZrO<sub>2</sub>-SiO<sub>2</sub> phase system at temperatures below 1687°C, although this phase was not detected by XRD.

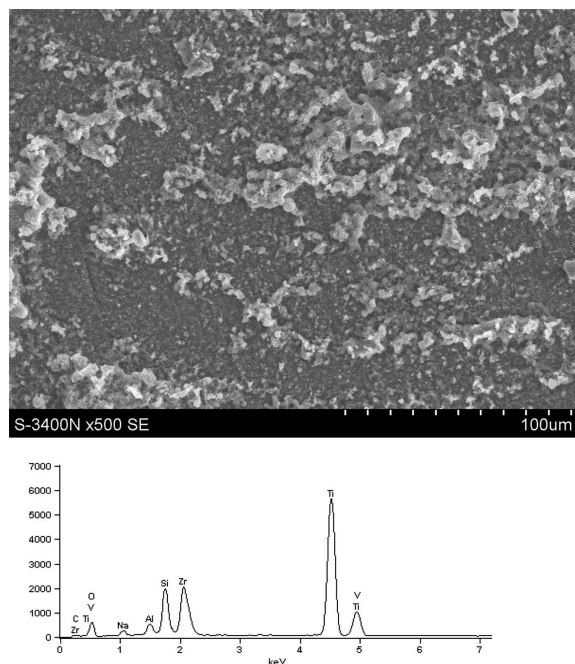


Fig. 6. The SEM image and the EDX spectrum of sample D1 sample

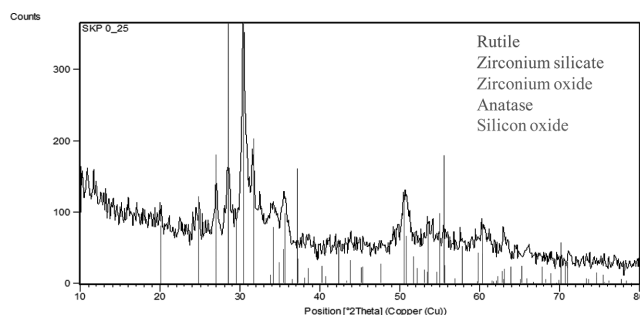


Fig. 7. XRD pattern of sample D1

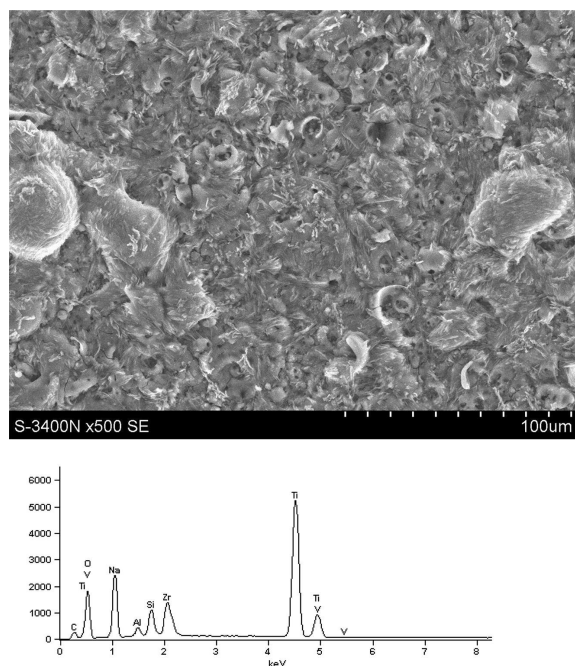


Fig. 8. The SEM image and the EDX spectrum of E2 sample

Further increase of the amount of NaOH to  $50 \text{ g dm}^{-3}$  significantly improve the morphology of the obtained layers. Its structure is fluctuated and porous. It's covered with oxide film and locally there are needle-shaped particles. The changes caused by increase of voltage (sample E2 anodised at 250 V) are not evident, surface of sample E2 seems to be more porous and fluctuated but roughness of sample E1 is larger than E2 (Fig. 8), and equals 3,94 and 3,06 respectively, but those aren't the greatest values among all examined samples (see D2 –  $R_a = 4.28 \mu\text{m}$  Fig. 11). Whereas, atomic ratios Zr/Si for samples E1 and E2 equal 0,99 and 0,96 respectively (Table 3). This value corresponds to atomic ratio of zirconium to silicon in  $\text{ZrSiO}_4$ . On the XRD pattern peaks of  $\text{ZrSiO}_2$  and  $\text{ZrO}_2$  are seen. Here, peaks from  $\text{SiO}_2$  are absent. It could be connected with hydrolysis, but in case of sample D the amount of newly formed  $\text{Na}_2\text{SiO}_3$  was smaller than when bath E was used. When amount of added NaOH equals  $10 \text{ g dm}^{-3}$  the amount of formed sodium silicate, due to hydrolysis, is small. With increasing alkalinity of the solution (increase of amount NaOH:  $50 \text{ g dm}^{-3}$ ) greater amount of sodium silicate can be formed. The presence of  $\text{ZrSiO}_4$  on the surface of sample was not earlier examined, there are papers concerning  $\text{ZrO}_2$  [14] or  $\text{SiO}_2$  [15] incorporation.

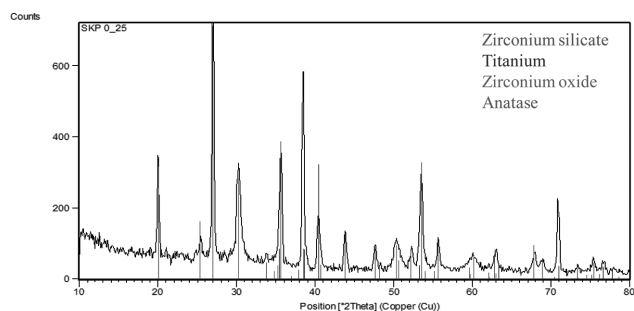


Fig. 9. XRD pattern of sample E2

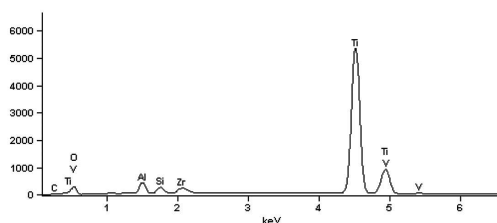
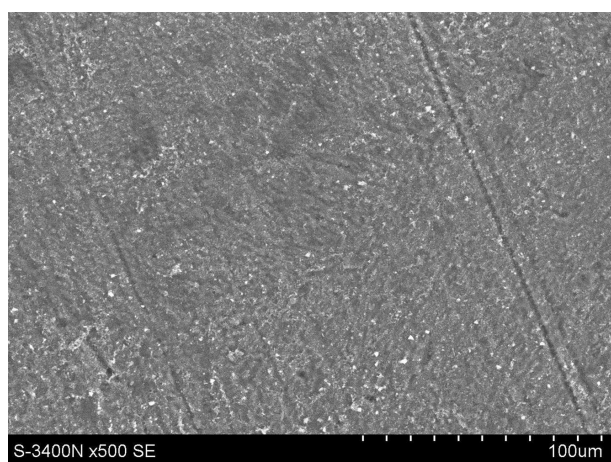


Fig. 10. The SEM image and the EDX spectrum of F2 sample

When samples were oxidized in bath F – ( $\text{ZrSiO}_4$ :  $200 \text{ g dm}^{-3}$  and NaOH:  $5 \text{ g dm}^{-3}$ ) obtained layers are relatively smooth with same particles on the surface (Fig. 10). Here, when greater voltage was applied more particles were incorporated on the surface, but their amount it still relatively low in comparison to surfaces of samples E.

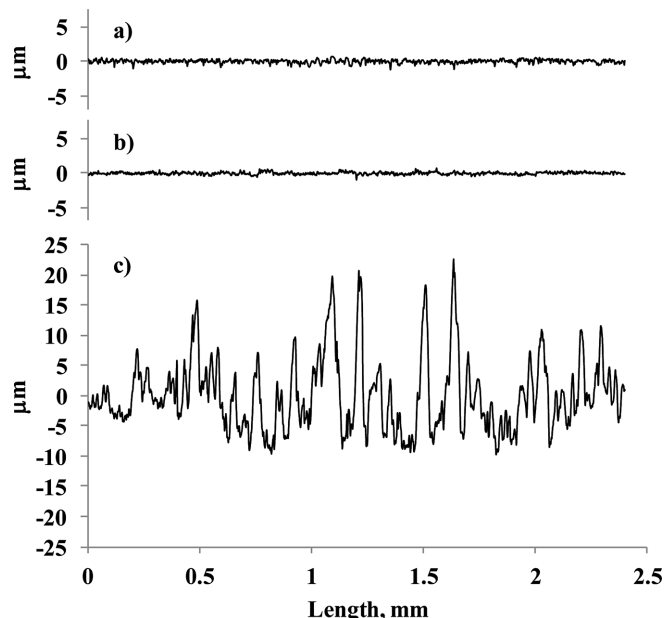


Fig. 11. The exemplary surface profiles obtained for a) grinded surface b) sample C2 c) sample D2

#### 4. Conclusions

In this paper preliminary investigations on possibility of zirconium silicate incorporation into oxide film on Ti-6Al-4V alloy were presented. It was found that with increasing of NaOH concentration amount of incorporated zirconium silicate also increase. Increasing of  $\text{ZrSiO}_4$  concentration also improve the process but changes are not significant. As the result of PEO process oxide layers were obtained which could represent multiphase or composite system. Further detailed examinations of obtained oxide layers are in progress, and will be presented in the next paper.

#### Acknowledgements

This work was supported by the Polish Ministry of Science and Education under research project no. IP 2010 0377 70.

#### REFERENCES

- [1] M. Long, H.J. Rack, *Biomaterials* **19**, 1621 (1998).
- [2] I. Apachitei, A. Leoni, A.C. Riemslog, L.E. Apachitei-Fratila, J. Duszczyk, *Applied Surface Science* **257**, 6941 (2011).
- [3] M. Shokoufar, C. Dehghanian, M. Montazeri, A. Baradaran, *Applied Surface Science* **258**, 2416 (2012).
- [4] C. Kuphasuk, Y. Oshida, C.J. Andres, S.T. Hovijitra, M.T. Barco, D.T. Brown, *The Journal of Prosthetic Dentistry* **85**, 195 (2001).

- [5] S.R. Sousa, M.A. Barbosa, *Biomaterials* **17**, 397 (1996).
- [6] C. Piconi, G. Maccauro, *Biomaterials* **20**, 1 (1999).
- [7] Y. Ramaswamy, C. Wu, A. Van Hummel, V. Combes, G. Grau, H. Zreiqat, *Biomaterials* **29**, 4392 (2008).
- [8] Y. Ramaswamy, C. Wu, A. Van Hummel, V. Combes, *Biomaterials* **29**, 4392 (2008).
- [9] H. Hu, X. Liu, C. Ding, *Surface and Coating Tech.* **204**, 3265 (2010).
- [10] A.M. Pietak, J.M. Reid, M.J. Stott, M. Sayer, *Biomaterials* **28**, 4023 (2007).
- [11] X.L. Zhang, H.Zh. Jiang, H.Zh. Yao, D.Zh. Wu, *Corrosion Science* **52**, 3465 (2010).
- [12] B. Ferrari, R. Moreno, *Journal of the European Ceramic Society* **30**, 1069 (2010).
- [13] E. Matykina, R. Arrabal, F. Monfort, P. Skeldon, G.E. Thompson, *Applied Surface Science* **255**, 2830 (2008).
- [14] F. Samanipour, M.R. Bayati, F. Golestani-Fard, H.R. Zargar, A.R. Mirhabibi, V. Shoaie-Rad, S. Abbasi, *Materials Letters* **65**, 926 (2011).
- [15] A.M. Pietak, J.W. Reid, M.J. Scott, M. Sayer, *Biomaterials* **28**, 4023 (2007).

*Received: 20 March 2013.*